Research Paper

Experimental investigations into power generation with low grade waste heat and R245fa Organic Rankine Cycles (ORCs)

L. Li [a], Y.T. Ge [a,*], X. Luo [b], S.A. Tassou [a]

[a] RCUK National Centre for Sustainable Energy Use in Food Chains (CSEF), Institute of Energy Future, Brunel University London, Uxbridge, Middlesex UB8 3PH, UK
[b] National Key Laboratory of Science and Technology on Aero Engines Aero-Thermodynamics, The Collaborative Innovation Centre for Advanced Aero-Engine of China, Beihang University, Beijing 10191, China

ABSTRACT

In this study, experimental research was conducted to investigate the performance of a small-scale Organic Rankine Cycle (ORC) system utilising low grade heat sources to generate electric power at different operating conditions. The experiment setup consisted of typical ORC system components, such as a turboexpander with high speed generator, finned-tube condenser, ORC pump and plate evaporator. R245fa was selected as a working fluid in the experimental system, considering its appropriate thermosphysical properties for the ORC system and low ozone depletion potential (ODP). At constant heat sink (ambient) parameters, extensive experiments were carried out to examine the effects of various important parameters including heat source temperature and working fluid pump speed etc. on system performance. Results showed that at a fixed working fluid speed, the thermal efficiency of the tested ORC system could be improved with an increased heat source temperature. On the other hand, at a constant heat source temperature, the working fluid pump speed could be optimised to maximise system thermal efficiency. Both the heat source temperature and ORC pump speed were found to be important parameters in determining system thermal efficiency and the component operations. The experimental outcomes can instruct future optimal system design and controls.

© 2017 The Author(s). Published by Elsevier Ltd. This is an open access article under the CC BY license (http://creativecommons.org/licenses/by/4.0/).

1. Introduction

The extensive consumption of fossil fuels worldwide has been contributing increasingly towards global warming, air pollution and the imminent energy crisis. One of the challenges of the 21st century is to tackle the risks arising from excessive CO_2 emissions by replacing fossil fuels with renewable energy and recovered waste heat. The waste heat sources can be divided into three main categories according to their temperature range: high temperature (>650 °C), medium temperature (230–650 °C) and low temperature (<230 °C) [1]. However, statistics have shown that more than 50% of industrial waste heat is within the low-grade range [2]. One highly recommended strategy for recovering low-grade waste heat for power generation is to utilise appropriate thermodynamic power cycles such as Organic Rankine Cycles (ORCs) [3,4].

The ORC functions similarly to a Clausius-Rankine steam power plant, but instead uses an organic working fluid such as R245fa, which is able to condense at a lower pressure and evaporate at a higher pressure. Many studies have shown that different working fluids can be applied in ORC systems based on their appropriate thermophysical properties, safety, cost and environmental impact etc. [5–8]. Nevertheless, there is no working fluid that can meet all the above requirements. Therefore, various named methods such as the bucket effect and spinal point were used to balance the impact and optimise selection [9]. Subsequently, eight organic working fluids including HFE7000, R245fa and R134a etc., which have been mostly applied and investigated in the past decade, were chosen to evaluate, compare and finally be ranked. Moreover, the author acknowledged that an accurate ORC working fluid selection must be driven by a specific heat source [10]. For instance, R134a was believed to be the most suitable working fluid for small-scale solar ORC applications [11]. In applications of geothermal electricity with ORC systems, R123 or n-pentane might be the best choice for the working fluid [12]. On the other hand, since these ORC working fluids are all pure substances and operate under subcritical cycles, the temperature mismatch between the hot and cold side fluids in the high pressure side heat exchanger will increase the irreversible loss and thus affect system efficiency. In such circumstances, using zeotropic mixtures such as R245fa/R152a as ORC working fluids could be more feasible options [13,14].

---

* Corresponding author.
  E-mail address: Yunting.Ge@brunel.ac.uk (Y.T. Ge).

Nomenclature

Cp	specific heat capacity (kJ/kg K)	*Subscripts*	
H	enthalpy (J/kg)	all	overall
K	thermal conductivity (W/m K)	e	electrical
$\dot{m}$	mass flow rate (kg/s)	ev	evaporator
P	pressure (pa)	f	fluid
Q	heat transfer rate (W)	in	inlet
R	rotation speed (RMP)	is	isentropic
P	pressure (pa)	m	mechanical
Q	heat transfer rate (W)	P	pump
T	temperature (^{0}C)	s	heat source
ΔT	temperature difference (K)	sh	superheat
W	work input/output (W)	T	turbine
η	efficiency (–)	th	thermal
ρ	density (kg/m^3)		
μ	kinematic viscosity (mm^2/s)		

In an ORC system, the expander is a critical component and its performance can determine overall system thermal efficiency. Similar to compressors in refrigeration systems, the ORC expanders can also be classified into two types: positive displacement such as scroll, vane and screw, and speed ones including turboexpander or turbine. In an application of the micro-CHP system with integrated biomass boiler and HFE7000 ORC, a vane type of expander was employed for experimental investigation [15]. In such a system, the biomass boiler heated pressurised water flow to around 125 °C and then indirectly evaporated and superheated the ORC fluid. However, the system power generation and thermal efficiency were 0.861 kW$_e$ and 1.41% respectively, both relatively low but can be potentially improved by better expander and ORC evaporator design etc. For a given heat source temperature of 105 °C, experiments and simulation on an R245fa ORC with scroll expanders of different displacements were carried out with a maximum system thermal efficiency of 3.2% [16]. The effects of displacement values on the expander and system efficiencies may be different. A R123 ORC test rig with a screw expander was set up to investigate the effect of various inlet vapour dryness on the expander efficiency [17]. The test results demonstrated that the increased inlet vapour dryness could enhance the expander power output but would reduce both the expander volumetric and overall efficiencies. Compared with the scroll and screw expanders in an ORC system, a turboexpander or turbine has a number of advantages in terms of manufacturability, unit weight, stability and efficiency [18]. It was reported that when a turboexpander or turbine was used as an expander in an R123 ORC system, the expander isentropic and system thermal efficiencies could be improved compared to its scroll or screw counterparts [19]. The turboexpander was deemed suitable for a small-scale ORC system application.

Both air-cooled and water-cooled condensers are commonly utilised in ORC systems to release heat from the systems to heat sinks. The water cooled condenser is relatively compact and high efficiency but usually needs to have an extra cooling mechanism to cool down the warm water. The air cooled condenser is normally a finned-tube with enhanced flexibility but a larger size, and therefore needs to be designed optimally for both hydraulic and heat transfer behaviours [20].

It is known from the literature that the heat source temperature is an important parameter in determining the appropriate selections of working fluids in an ORC system. However, the detailed effects of the heat source temperature on the expander efficiency and system performance need to be further investigated. In addition, the operation of an ORC system is more complicated than that of a conventional refrigeration system. An ORC liquid pump can take an important role in the system operations and controls but this also needs further investigation. Accordingly, this paper introduces a small-scale R245fa ORC system test rig in which a turboexpander and air cooled finned-tube condenser were utilised. The effects of heat source temperatures and R245fa liquid pump speeds on the expander efficiency and system performance have been measured and analysed. The research outcomes can contribute significantly to the ORC fluid selections, system component designs and system controls.

2. Experimental system and facilities

A small-scale R245fa ORC test rig was developed in the laboratory at Brunel University, as shown in Fig. 1. The test system consisted of two operational loops, namely heat source and ORC. In the heat source loop, the exhaust gas from an 80 kW$_e$ CHP unit as shown in Fig. 2c was recovered to heat a heat transfer medium, thermal oil, through an exhaust gas-thermal oil boiler. The hot thermal oil was then circulated via an oil circulation pump to the R245fa evaporator and flowed back to the oil boiler to be heated again. The thermal oil flow rate was controlled by a variable frequency drive attached to the oil pump while the thermal oil (heat source) temperature was modulated by means of the CHP power output controls [21]. To facility the heat transfer and energy balance analysis of the R245fa evaporator, the thermal oil properties were correlated from the manufacture's data for the thermal oil temperature ranging from 0 °C to 340 °C:

For density (kg/m^3),

$$\rho = -0.65035606\,t + 875.94428 \qquad (1)$$

For specific heat capacity (kJ/kg°K),

$$Cp = 0.0036446769\,t + 1.8087169 \qquad (2)$$

For thermal conductivity (W/m°K),

$$k = -7.2360691 \times 10^{-5}\,t + 0.13570055 \qquad (3)$$

For kinematic viscosity (mm^2/s),

$$\mu = 27604.397\,t^{-1.879364} \qquad (4)$$

The R245fa ORC loop consisted of a number of essential components: an oil heated plate-type evaporator, R245fa turboexpander/turbine and power generator, finned-tube air cooled condenser, liquid receiver and liquid pump. The liquid R245fa was heated by the evaporator to a superheated vapour and was
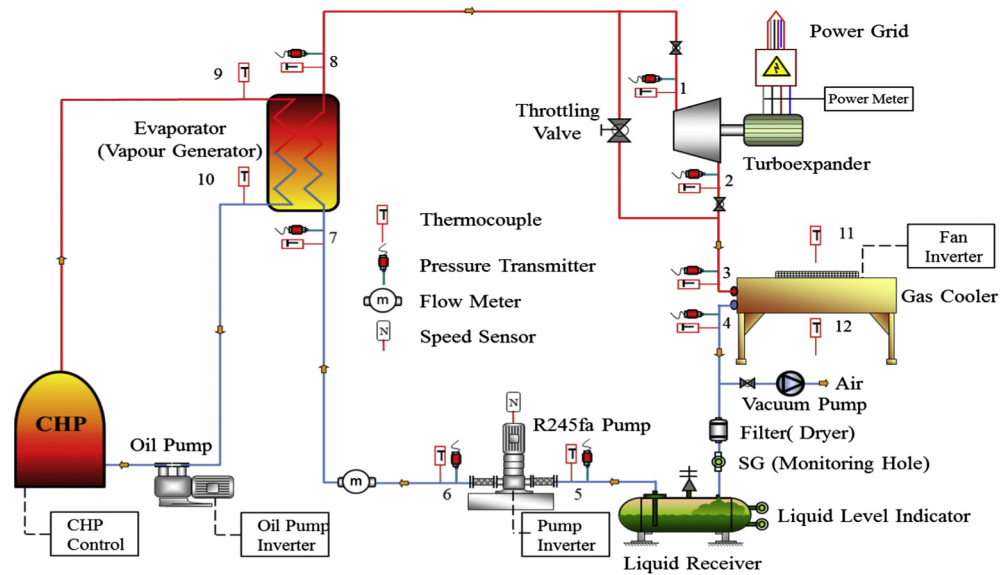
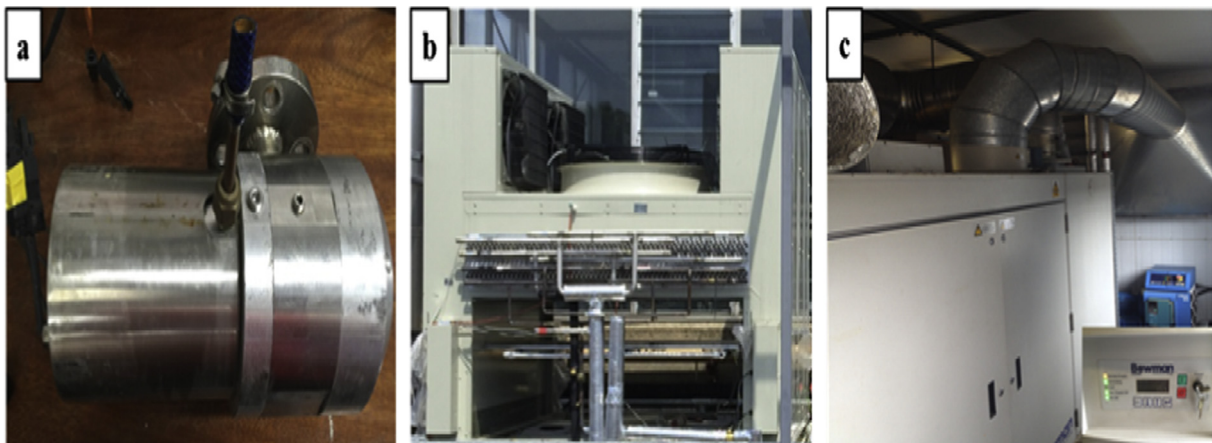Fig. 1. R245fa ORC experimental system and facilities.

Fig. 2. Photographs of the system components. (a) Turboexpander, (b) finned-tube air cooled condenser, (c) 80 kW$_e$ CHP unit.

then expanded in the turboexpander to generate power. The turboexpander, which is shown in Fig. 2a, was integrated with a high speed and permanent magnet synchronous generator. The power generator was driven by an ABB inverter and connected to the electric grid in the campus. In addition, a bypass valve was installed in parallel to the expander to bypass a fraction of R245fa vapour or be used as an expansion device when necessary. From the expander outlet, the R245fa low pressure vapour flowed directly into the finned-tube air cooled condenser and was condensed into sub-cooled liquid before pouring into the liquid receiver. As shown in Fig. 2b, the condenser was suspended tightly between two upright metal frames of a purposely built test facility. A propeller air fan with variable speed control was installed above the heat exchanger to maintain a passage of fixed air flow. Above this, there were a number of smaller air fans installed oppositely along the direction of pipe length, which would be switched on if the air on temperature was controlled to be higher than ambient. As such, part of the hot exhaust air would flow back through the return air tunnels, the return air grills and finally mix with the lower temperature ambient air flow. If the mixed air flow temperature was still lower than the designed air on temperature, an electric air heater installed just below the heat exchanger was controlled to turn on in order to

maintain the air on temperature. From the liquid receiver, the working fluid was then pumped back to the evaporator to continue another operation cycle. Similar to the condenser fan, the liquid pump speed could also be controlled by a frequency drive inverter which could modulate the working fluid flow rate and operating pressures in the ORC cycle.

To measure extensively the performance of the system and its main components, a temperature sensor and a pressure transducer were installed at the inlet and outlet of each component in the ORC system. In addition, the thermal oil and air flow inlet and outlet temperatures were also measured respectively at the evaporator and condenser. The measurements also included the expander power generation and R245fa mas flow rate. For these measurement instruments, each temperature was measured by a K-type 310 stainless steel sheath thermocouple with accuracy of ±0.5 °C. A pressure transducer with 0–25 bar range, ±0.3% accuracy and a 0.5 s response time was applied for the pressure measurement at each point. All thermocouples and pressure transducers were inserted into the pipelines and at locations close to each component. A twin tube type mass flowmeter was used to measure the liquid mass flow of R245fa after the pump. The flowmeter could measure mass flow in the range of 0–6500 kg/h with an accuracy

Table 1
Main measurement instruments used in the experimental system.

Parameters	Type	Range	Accuracy
Temperatures	K-type thermocouple	(−10) to 1100 °C	±0.5 °C
Pressures	AKS 32	0–25 bar	±0.3%
Flowmeter	Twin tube type	0–6500 kg/h	±0.15%
Speed sensor	Laser sensor	50–6000 RPM	±0.75%
Power meter	Digital multimeter	1 mW–8 kW	±0.8%
Air flow meter	TA465	1.27–78.7 m/s	0.15 m/s

of ±0.15%. A laser speed sensor was used to measure RPM of pump shaft with an accuracy of ±0.75% at full scale of 50–6000 RPM. A power meter was used for electric power measurement from output of the turboexpander within an accuracy class of ±0.8%. All meter transient output signals of the experimental data were transmitted to computer by a National Instruments data logger system and recorded for further analysis. In general, the detailed specifications of the main measurement instruments used in the system are listed in Table 1.

3. Results and discussions

After the test rig was setup, a series of experiments were conducted to evaluate the performance of the ORC system with turboexpander at different heat source (thermal oil) temperatures and running speeds of ORC pump. The thermal oil temperatures were controlled from 138 °C to 156 °C by modulating the CHP system power outputs while the ORC pump speeds were varied from 630 RPM to 779 RPM by changing the ORC pump motor frequencies. These settings were to guarantee the turbine inlet temperatures and pressures to be within their maximum limitations during the tests which were set as 110 °C (120 °C for a short period) and 14 bar respectively by the turbine manufacture. Temperatures, pressures, mass flow rate and other auxiliary data of R245fa and thermal oil were measured and recorded by a dedicated data logger when the system was at steady state. All relevant fluid thermophysical properties such as enthalpy and entropy etc were calculated by REFPROP 8.0 software [22] based on the average measured temperature and pressure at each cycle point.

3.1. The effect of the heat source temperature swing

To examine the effect of heat source (thermal oil) temperature on the ORC system performance, the thermal oil temperature was controlled to vary from 135 °C to 160 °C by modulating the CHP power outputs. In the meantime, as listed in Table 2, all other operating parameters such as thermal oil flow rate, R245fa pump speed, condenser air flow rate and ambient air temperature were maintained constants.

Subsequently, the variations of cycle point and oil outlet temperatures with heat source (thermal oil) temperatures were measured and are shown in Fig. 3. The measurements demonstrated that the thermal oil evaporator outlet temperature and R245fa fluid temperatures at turbine inlet and outlet and condenser inlet all increased with higher heat source temperatures. When analysing solely the turbine inlet temperature, it is found that the temperature increased about linearly with higher heat source temperature when it was greater than 140 °C. However, when the heat source temperature was below 140 °C, the R245fa temperature just increased slightly. This illustrates that when the heat source temperature was at 130 °C the R245fa fluid was not evaporated completely and higher heat source temperature was needed to ensure a dry R245fa fluid at the evaporator outlet or the turbine inlet. Meanwhile, both condenser and pump outlet temperatures were not affected much by the heat source temperatures considering of constant heat sink parameters and pump speed. In addition, it is noted that the condenser outlet temperature or pump inlet temperature was more or less the same as the pump outlet temperature considering the liquid pumping process involved. Precisely, for dry turbine operations, when the heat source temperature increased from 141 °C to 155 °C, the temperatures of thermal oil outlet, turbine inlet, turbine outlet and condenser inlet increased about 9.0 K, 25.6 K, 27.8 K and 27.8 K respectively.

The variations of cycle point pressures with heat source temperatures are depicted in Fig. 4. Obviously, the working fluid pressures can be separated into two groups of high and low pressure sides. The high pressure side includes the pressures of pump outlet, evaporator inlet, and evaporator outlet and turbine inlet while the low pressure side includes the pressures of turbine outlet, condenser inlet, condenser outlet and pump inlet. The measurements showed that the working fluid pressures at high pressure side increased with higher heat source temperature while those at low pressure side were not affected much by the heat source temperatures. Subsequently, the pressure ratios of turbine inlet and outlet increased with higher heat source temperatures. In addition, the cycle point pressures at each pressure side were different indicating the diverse fluid pressure drops through the connection pipes, fittings and components with the maximum and minimum pressure points at the pump outlet and inlet respectively in the system. In percentage, when the heat source temperature increased from 141 °C to 155 °C, the cycle point pressures of ORC pump outlet, evaporator inlet and outlet, turbine inlet and outlet, condenser inlet and outlet, and ORC pump inlet amplified 7.41%, 7.46%, 7.49%, 7.89%, 4.12%, 4.38%, 1.34% and 0.38% respectively.

At the fixed R245fa liquid pump speed, the R245fa mass flow rate was measured constantly as 0.25 kg/s at different heat source temperatures. Based on also the measured temperature and pressure at each component inlet and outlet, the pump power and evaporator and condenser capacities could be calculated at different heat source temperatures, as shown in Fig. 5. In addition, the actual turbine power output was measured directly with an installed power meter which is also presented in the same Figure. The higher heat source temperature enhanced the heat transfer of the evaporator and thus leading to higher evaporator heat capacity. As shown in Fig. 3, the higher heat source temperature could also increase the working fluid temperature at the condenser inlet but unchanged condenser outlet temperature which would therefore increase the condenser heat output. In addition, as depicted in Fig. 4, the higher heat source temperature raised the working fluid pressure ratio of turbine inlet and outlet and thus the turbine power output. However, the pump power input had the smallest increase with the higher heat source temperature compared to others considering the its minimum effect on the pump inlet and outlet parameters. Quantitatively, when the heat source temperature increased from 145 °C to 155 °C, the percentage increase rates of turbine power output, evaporator heat input, condenser heat output and pump power input were 13.6%, 12.7%, 9.4% and 6.6% respectively.

The isentropic efficiencies of turbine and liquid pump are calculated in Eqs. (5) and (6) respectively. The variable subscript numbers in these equations are corresponding to the ones indicated in Fig. 1. As listed in Eq. (7), the turbine overall efficiency can be calculated as a production of isentropic, mechanical and electrical efficiencies. The overall efficiency can also be calculated as the ratio of measured turbine power output and the turbine isentropic power output. Accordingly, if the mechanical efficiency is assumed as constant 0.98, the electrical efficiency can be calculated. When mechanical and electrical efficiencies are not included in the calculations of overall efficiency for the pump, the power input of the pump can be calculated in Eq. (8). The system thermal efficiency can therefore be calculated as Eq. (9).

Table 2
The operating conditions for the experiment set up of thermal oil temperature swing.

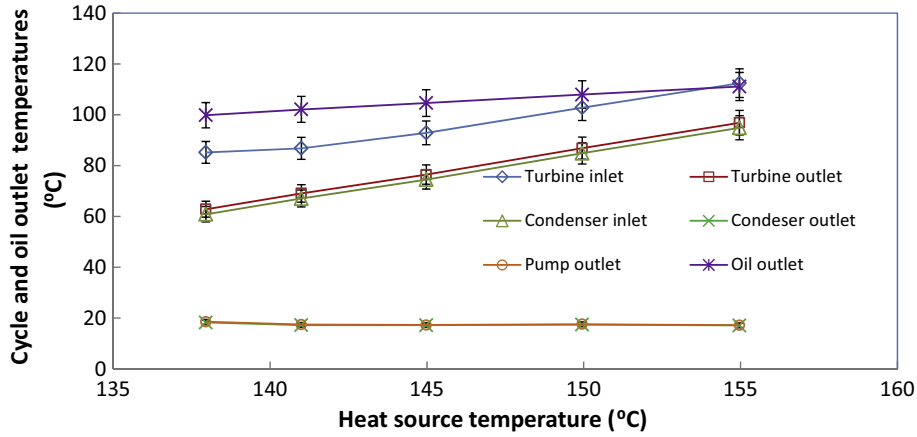| Oil temperature (°C)	Oil flow rate (kg/s)	R245fa pump speed (RPM)	Condenser flow rate percentage of max fan speed (%)	Ambient air temperature (°C)
135–160	0.65	680	100	17

Fig. 3. Variations of cycle point and oil outlet temperatures (including 5% error bars) with heat source (thermal oil) temperatures.
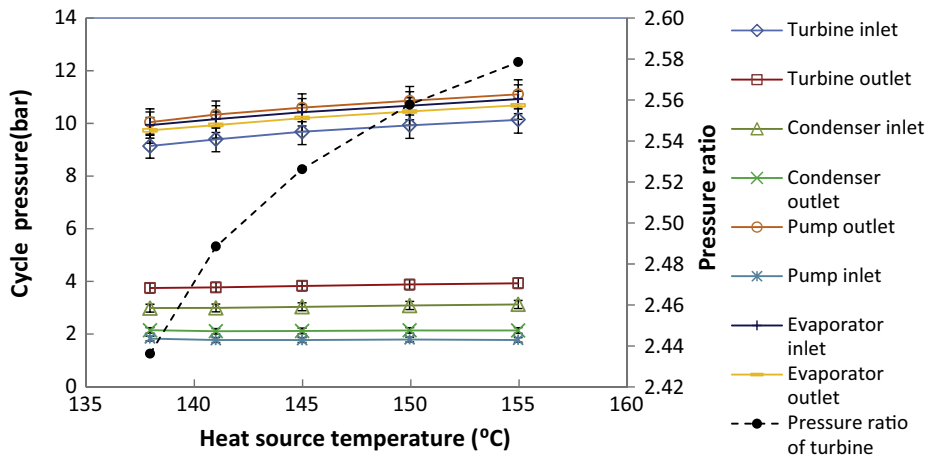

Fig. 4. Variations of cycle point pressures (including 5% error bars)with heat source (thermal oil) temperatures.
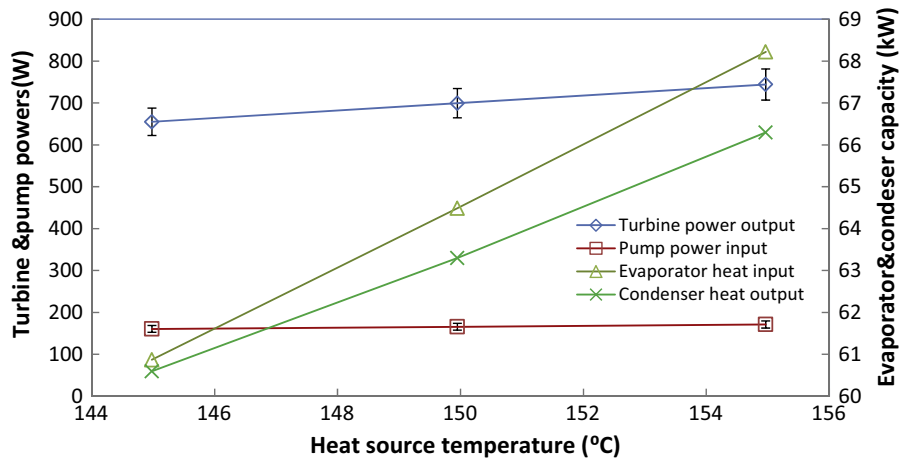
Fig. 5. Variations of turbine and pump powers (including 5% error bars) and evaporator and condenser capacity with heat source (thermal oil) temperatures.

$$\eta_{T,is} = \frac{(h_1 - h_2)}{(h_1 - h_{2,is})} \tag{5}$$

$$\eta_{P,is} = \frac{(h_6 - h_5)}{(h_{6,is} - h_5)} \tag{6}$$

$$\eta_{T,all} = \eta_{T,is}\eta_{T,m}\eta_{T,e} = \frac{W_T}{\dot{m}_f(h_1 - h_{2,is})} \tag{7}$$

$$W_P = \dot{m}_f(h_6 - h_5) \tag{8}$$

$$\eta_{th} = \frac{W_T - W_P}{Q_{ev}} \tag{9}$$

To demonstrate, the turbine and system thermal efficiencies at different heat source temperatures are calculated and depicted in Fig. 6. As presented in Fig. 4, the turbine pressure ratio increased with higher heat source temperature leading to higher turbine isentropic efficiency and also system thermal efficiency. However, the overall turbine efficiency doesn't change much with different heat source temperatures. In percentage, when the heat source temperature increases from 145 °C to 155 °C, 14.38%, 1.08%and 3.44% are increased for the turbine isentropic, overall and system thermal efficiencies respectively. It is noted that the actual turbine power output and system thermal efficiency are much lower than expected which can be explained by the following reasons: (1) the turbine pressure ratio is low due to extra high pressure drop between turbine outlet and condenser inlet; (2) the turbine isentropic and electrical efficiencies are both low indicating that further turbine design improvements are expected.

3.2. The effect of the ORC pump speed swing

As shown in Fig. 1, an ORC liquid pump was installed after the liquid receiver. The pump speed could be controlled so as to modulate the ORC fluid mass flow rate and pressure at the turbine inlet. To examine the effects of variable pump speeds on the system performance, a test matrix of ORC pump speed swing was designed and is listed in Table 3. As seen in the Table, the ORC pump speed was varied from 630 to 779 RPM while other parameters such as thermal oil (heat source) temperature and flow rate and condenser air (heat sink) flow rate and temperature were maintained constants.

Based on the test matrix set up in Table 3, the variations of cycle point and oil outlet temperatures, ORC mass flow rates with ORC pump speeds were measured and are plotted in Fig. 7. It is understandable that the ORC mass flow rate increased with ORC pump

speed which could therefore enhance the heat transfer for the heat exchangers in the system including evaporator and condenser. This would emulate a higher heating capacity of each heat exchanger including the evaporator such that the thermal oil outlet temperature decreased with ORC pump speed. Even so, the ORC evaporator outlet (turbine inlet) temperature was lower with increased ORC pump speed due to the fixed heat source parameters. It is also noticed that the turbine inlet temperature decreased almost linearly with ORC pump speed when it was less than 730 RPM and flattened when the pump speed increased further. This indicates that the ORC was at saturated state and the heat source capacity was not powerful enough to superheat the ORC fluid in the evaporator when the pump speed was higher than 730 RPM. The decreased ORC fluid temperature at turbine inlet lowered down the fluid temperature at the turbine outlet and thus condenser inlet. On the other hand, the ORC fluid temperatures at condenser outlet (pump inlet) and pump outlet increased with ORC pump speed because of the constant heat sink parameters. Subsequently, under such heat source and sink conditions, the ORC pump speed should not be higher than 730 RPM to ensure dry fluid to flow into the turbine. Quantitatively, when the ORC pump speed increased from 630 RPM to 730 RPM, the temperatures of thermal oil outlet, turbine inlet, turbine outlet and condenser inlet decreased approximately by 1.3 K, 18.9 K, 21.7 K and 21.9 K respectively. On the contrary, the ORC mass flow rate, ORC temperatures at condenser outlet and pump outlet increased 14.4%, 2.3 K and 2.5 K each.

The effects of varied ORC pump speeds on the cycle point pressures were measured and are plotted in Fig. 8. The pressure ratios of turbine inlet and outlet are calculated and also presented in this Figure. Clearly, the cycle point pressures can be classified into two groups based on their pressure magnitudes. The high pressure group includes the points at the ORC pump outlet, evaporator inlet and outlet and turbine inlet while the low pressure group consists of the locations at turbine outlet, condenser inlet and outlet and pump inlet. The pressure difference between two neighbour points in each group presented the pressure drop through the relevant pipe line or component. The largest pressure drop happened across the condenser followed by the pipework and fittings between turbine outlet to condenser inlet and then over the evaporator. It is reasonable that the ORC pump outlet pressure increased with pump speed which led all other cycle point pressures to increase with different scales. In percentage, when the ORC pump speed increased from 630 RPM to 730 RPM, the cycle point pressures of ORC pump outlet, evaporator inlet and outlet, turbine inlet and outlet, condenser inlet and outlet, and ORC pump inlet amplified 7.97%, 7.80%, 7.82%, 7.44%, 9.66%, 8.36%, 7.64% and 5.93% respectively. However, the pressure ratio of turbine inlet and outlet
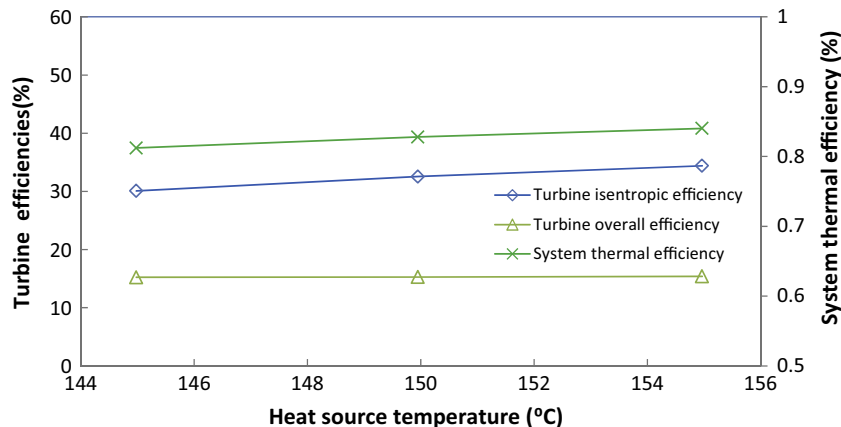
Fig. 6. Variations of turbine and system thermal efficiencies with heat source (thermal oil) temperatures.

Table 3
The operating conditions for the experiment set up of ORC pump speed swing.

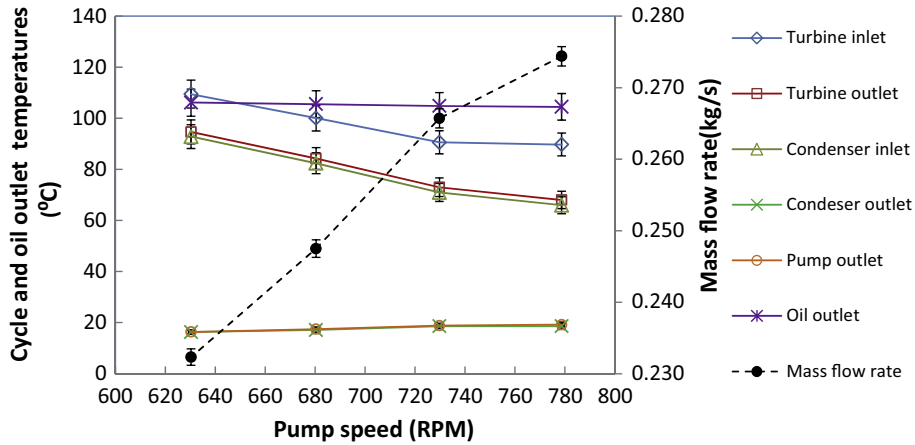| Oil temperature (°C)	Oil flow rate (kg/s)	R245fa pump speed (RPM)	Condenser flow rate Percentage of max fan speed (%)	Ambient air temperature (°C)
131.1	1.08	630–779	100	17.0

Fig. 7. Variations of cycle point, oil outlet temperatures (including 5% error bars), ORC mass flow rates (including 0.5% error bars) with ORC pump speeds.
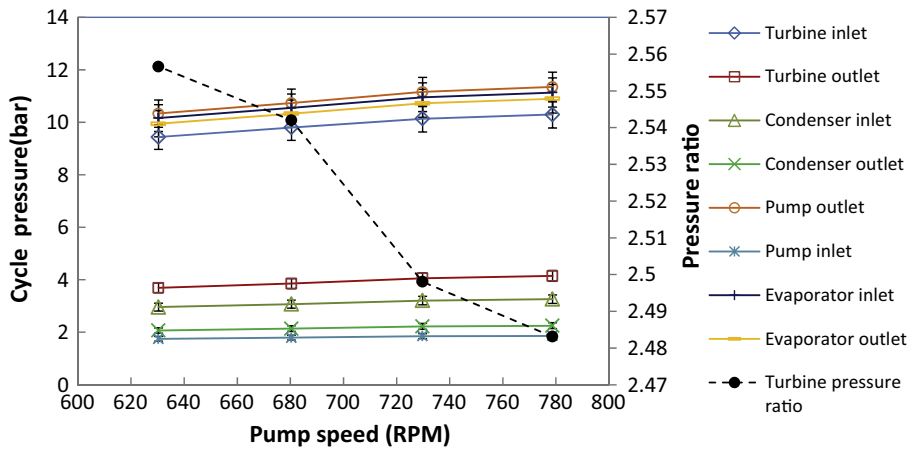

Fig. 8. Variations of cycle point pressures (including 5% error bars) with ORC pump speeds.

decreased with higher ORC pump speed considering the caused greater increase for the turbine outlet pressure.

The effects of varied ORC pump speeds on the turbine and pump powers and evaporator and condenser capacity are shown in Fig. 9. The turbine power outputs were measured directly while other performance results were calculated based on the measurements of ORC temperature, pressure and flow rate related to each component. As explained previously, the increased ORC pump speed would increase the ORC mass flow rate which enhanced the heat transfers in the ORC heat exchangers including evaporator and condenser. The evaporator heat input and condenser heat output therefore increased with ORC pump speed. In addition, with increased ORC pump speed, more ORC pump power input was required. On the other hand, although the turbine power out also increased with ORC pump speed but the increased rate is much less than those of others due to the reduced pressure ratio of turbine inlet and outlet and consequent turbine efficiency. It is noticed that when the ORC speed was above 730 RPM, the ORC fluid at turbine inlet would be wet which would reduce the increase rates of those powers and capacities. This again highlights the importance of ORC

pump speed limitation control in an ORC system. Generally, when the ORC pump speed increased from 630 RPM to 730 RPM, the turbine power output, evaporator heat input, condenser heat output and ORC pump power input increased by 4.92%, 1.66%, 3.18% and 24.49% respectively.

The effects of varied ORC pump speeds on the turbine isentropic and overall efficiencies and system thermal efficiency are shown in Fig. 10. As shown in Fig. 8, the pressure ratio of turbine inlet and outlet decreased with ORC pump speed which could directly result in lower turbine isentropic efficiency when increasing the pump speed. However, the turbine overall efficiency increased with ORC pump speed indicating that the turbine electrical efficiency increased more with greater ORC pump speed if the mechanical efficiency could be assumed as constant. As calculated in Eq. (9), the system thermal efficiency is a function of turbine power output, ORC pump power input and evaporator heat input which were all increased with ORC pump speed. However, the ORC pump power input had the largest increased rate such that the system thermal efficiency increased initially and then decreased at those ORC pump speed range. This demonstrated that there was an opti-
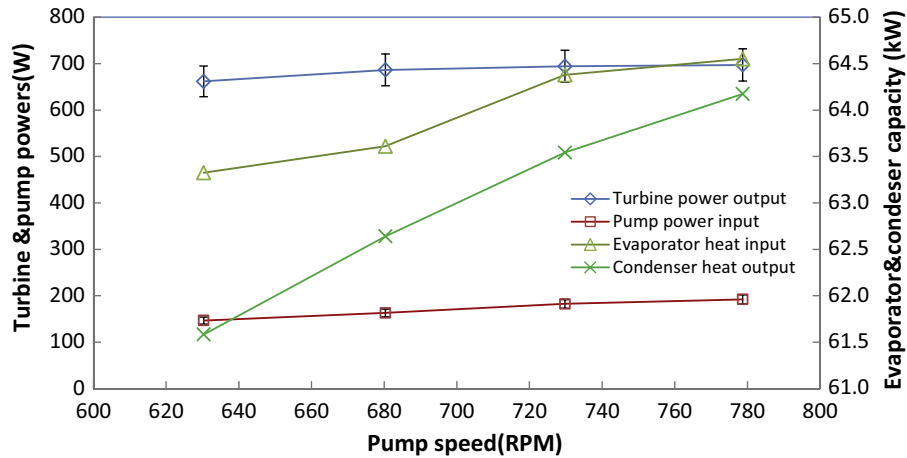
Fig. 9. Variations of turbine and pump powers (including 5% error bars) and evaporator and condenser capacity with ORC pump speeds.
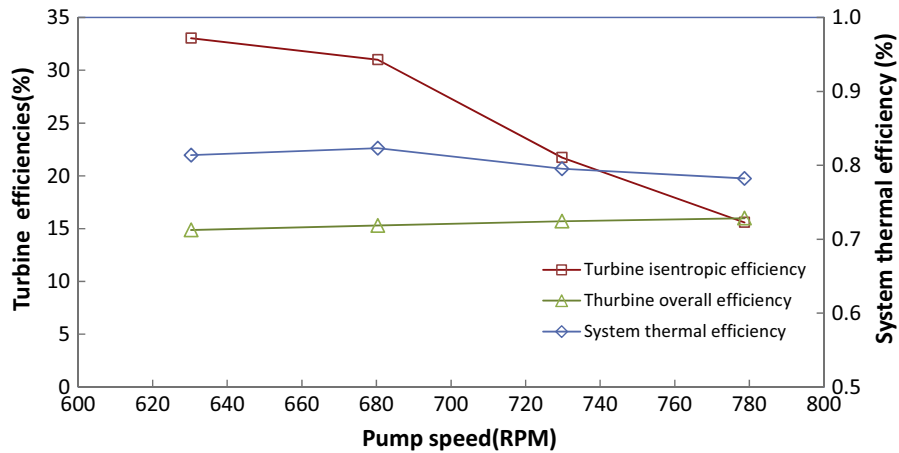

Fig. 10. Variations of turbine and system thermal efficiencies with ORC pump speeds.

mal ORC pump speed where the system thermal efficiency could be maximised.

4. Control strategies

The turbine inlet superheat (temperature) and pressure are two important parameters to be controlled in an ORC system considering their significant impacts on the system thermal efficiency. These two parameter controls will also ensure that the turbine temperature and pressure are always within their maximum limitations and dry turbine inlet conditions. As explained in Section 3.1, the heat source temperatures have major effects on both the turbine inlet temperature and pressure. The superheat at the turbine inlet is defined as the temperature difference of turbine inlet temperature and equivalent saturated vapour temperature based on turbine inlet pressure. From the test results, the relations between heat source temperatures and ORC fluid superheats at turbine inlet are shown in Fig. 11. It is seen that the heat source temperature should increase almost linearly if higher ORC fluid superheat at turbine inlet is needed which can be correlated as below:

$$t_s = 0.4711\Delta T_{sh,T} + 144.87 \qquad (10)$$

As demonstrated in Section 3.2, the ORC fluid pressure at turbine inlet is strongly affected by the ORC fluid pump speed such that the control function between these two parameters can be constructed. As depicted in Fig. 12, the ORC pump speed should increase near linearly if higher ORC fluid pressure at turbine inlet is required which can be correlated as the following equation:

$$R_P = 141.45P_{T,in} - 705.59 \qquad (11)$$

In practice, these two functions listed in Eqs. (10) and (11) can be used to control the ORC fluid superheat and pressure at turbine inlet respectively. For the superheat control, two sensing parameters of ORC fluid temperature and pressure at turbine inlet are needed to modulate the heat source temperature. Meanwhile, only one sensing parameter of ORC fluid pressure at turbine inlet is required to modulate the pump speed.

5. Conclusions

Over 50% industrial waste heats are currently classified as low-grade, with R245fa ORC power generation systems being conventional designs for low-grade energy conversions. However, further investigations are required for ORC system operation, control and optimisation. This paper reports experimental results on the effects of two important operating parameters including heat source temperature and ORC liquid pump speed on the performance of a small-scale low-grade R245fa ORC system. Several useful research outcomes have been obtained. These include:
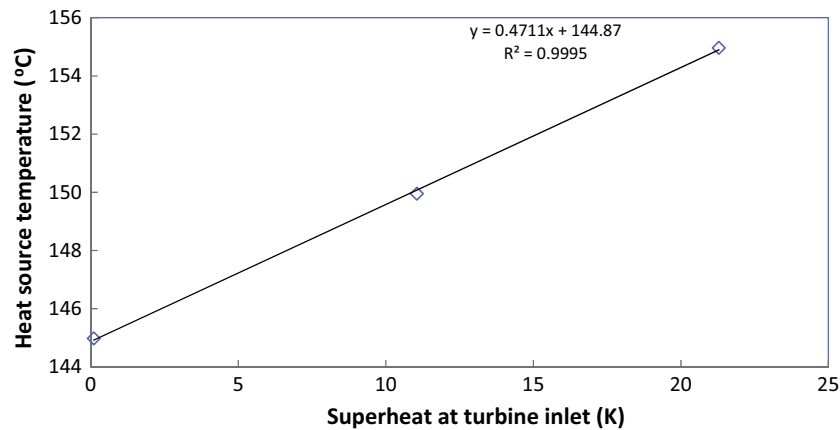
Fig. 11. Relations between heat source temperatures and ORC fluid superheats at turbine inlet.
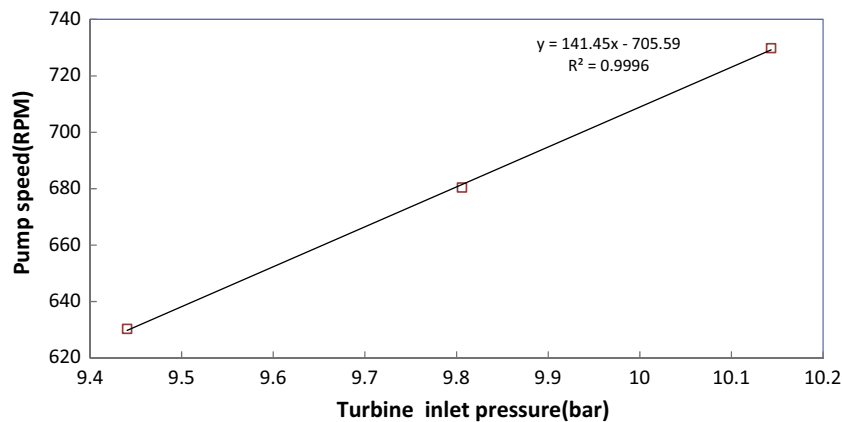

Fig. 12. Relations between ORC pump speeds and ORC turbine inlet pressures.

- At higher heat source temperatures, the temperatures of the heat source outlet, turbine inlet and outlet and condenser inlet all increased differently but the temperatures of the condenser outlet or pump inlet and pump outlet did not change much. In addition, all the cycle point pressures and the pressure ratio of turbine inlet and outlet increased at higher heat source temperatures.

- At higher heat source temperatures, the turbine power output, ORC pump power input, evaporator heat input, condenser heat output, turbine isentropic and overall efficiencies and system thermal efficiency all increased.

- At higher ORC pump speeds, the temperatures of thermal oil outlet, turbine inlet, turbine outlet and condenser inlet all decreased but the ORC mass flow rate, ORC temperatures at condenser outlet and pump outlet were all increased. In addition, all cycle point pressures were increased but the pressure ratio of turbine inlet and outlet was decreased.

- At higher ORC pump speeds, the turbine power output, ORC pump power input, evaporator heat input, condenser heat output and turbine overall efficiency all increased but the turbine isentropic efficiency decreased. There was an optimal ORC pump speed to obtain a maximum system thermal efficiency.

Furthermore, the ORC fluid superheat and pressure at the turbine inlet were found to be two important parameters which can be respectively controlled with heat source temperature and ORC pump speed.

References

[1] B.F. Tchanche, G. Lambrinos, A. Frangoudakis, G. Papadakis, Low-grade heat conversion into power using organic rankine cycles – a review of various applications, Renew. Sustain. Energy Rev. 15 (2011) 3963–3979.
[2] T.C. Hung, T.Y. Shai, S.K. Wang, A review of organic rankine cycles (ORCs) for the recovery of low-grade waste heat, Energy 22 (1997) 661–667.
[3] S. Lecompte, H. Huisseune, M. van den Broek, B. Vanslambrouck, M. De Paepe, Review of organic Rankine cycle (ORC) architectures for waste heat recovery, Renew. Sustain. Energy Rev. 47 (2015) 448–461.
[4] T. Yamamoto, T. Furuhata, N. Arai, K. Mori, Design and testing of the organic Rankine cycle, Energy 26 (2001) 239–251.
[5] J. Bao, L. Zhao, A review of working fluid and expander selections for organic Rankine cycle, Renew. Sustain. Energy Rev. 24 (2013) 325–342.
[6] O. Badr, S.D. Probert, P.W. O'Callaghan, Selecting a working fluid for a Rankine-cycle engine, Appl. Energy 21 (1985) 1–42.
[7] B. Saleh, G. Koglbauer, M. Wendland, J. Fischer, Working fluids for low-temperature organic Rankine cycles, Energy 32 (2007) 1210–1221.
[8] H. Chen, D.Y. Goswami, E.K. Stefanakos, A review of thermodynamic cycles and working fluids for the conversion of low-grade heat, Renew. Sustain. Energy Rev. 14 (2010) 3059–3067.
[9] G. Qiu, Selection of working fluids for micro-CHP systems with ORC, Renew. Energy 48 (2012) 565–570.
[10] Z.Q. Wang, N.J. Zhou, J. Guo, X.Y. Wang, Fluid selection and parametric optimization of organic Rankine cycle using low temperature waste heat, Energy 40 (2012) 107–115.

[11] B.F. Tchanche, G. Papadakis, G. Lambrinos, A. Frangoudakis, Fluid selection for a low-temperature solar organic Rankine cycle, Appl. Therm. Eng. 29 (2009) 2468–2476.

[12] H.D.M. Hettiarachchia, M. Golubovica, W.M. Worek, Y. Ikegami, Optimum design criteria for an organic Rankine cycle using low-temperature geothermal heat sources, Energy 32 (2007) 1698–1706.

[13] V. Le, A. Kheiri, M. Feidt, S. Pelloux-Prayer, Thermodynamic and economic optimizations of a waste heat to power plant driven by a subcritical ORC (Organic Rankine Cycle) using pure or zeotropic working fluid, Energy 78 (2014) 622–638.

[14] Y. Li, M. Du, C. Wu, S. Wu, C. Liu, Potential of organic Rankine cycle using zeotropic mixtures as working fluids for waste heat recovery, Energy 77 (2014) 509–519.

[15] G. Qiu, Y. Shao, J. Li, H. Liu, S.B. Riffat, Experimental investigation of a biomass-fired ORC-based micro-CHP for domestic applications, Fuel 96 (2012) 374–382.

[16] P. Gao, L. Jiang, L. Wang, R. Wang, F. Song, Simulation and experiments on an ORC system with different scroll expanders based on energy and exergy analysis, Appl. Therm. Eng. 75 (2015) 880–888.

[17] G. Xia, Y. Zhang, Y. Wu, C. Ma, W. Ji, S. Liu, H. Guo, Experimental study on the performance of single-screw expander with different inlet vapor dryness, Appl. Therm. Eng. 87 (2015) 34–40.

[18] W. Pu, C. Yue, D. Han, W. He, X. Liu, Q. Zhang, Y. Chen, Experimental study on Organic Rankine cycle for low grade thermal energy recovery, Appl. Therm. Eng. 94 (2016) 221–227.

[19] G. Pei, J. Li, Y. Li, D. Wang, J. Ji, Construction and dynamic test of a small-scale organic Rankine cycle, Energy 36 (2011) 3215–3223.

[20] Y.T. Ge, S.A. Tassou, Thermodynamic analysis of transcritical CO_2 booster refrigeration systems in supermarket, Energy Convers. Manage. 52 (2011) 1868–1875.

[21] Y.T. Ge, S.A. Tassou, I. Chaer, N. Suguartha, Performance evaluation of a tri-generation system with simulation and experiment, Appl. Energy 86 (2009) 2317–2326.

[22] E. Lemmon, M. Huber, M. McLinden, NIST REFPROP standard reference database 23. Version 8.0. User's guide. NIST, 2007.